

# Subtype-specific promoter-driven action potential imaging for precise disease modelling and drug testing in hiPSC-derived cardiomyocytes

Zhifen Chen<sup>1†</sup>, Wenying Xian<sup>2†</sup>, Milena Bellin<sup>3</sup>, Tatjana Dorn<sup>1</sup>, Qinghai Tian<sup>2</sup>, Alexander Goedel<sup>1</sup>, Lisa Dreizehnter<sup>1</sup>, Christine M. Schneider<sup>1</sup>, Dorien Ward-van Oostwaard<sup>3</sup>, Judy King Man Ng<sup>1</sup>, Rabea Hinkel<sup>1,4,5</sup>, Luna Simona Pane<sup>1</sup>, Christine L. Mummery<sup>3</sup>, Peter Lipp<sup>2</sup>, Alessandra Moretti<sup>1,4\*</sup>, Karl-Ludwig Laugwitz<sup>1,4\*</sup>, and Daniel Sinnecker<sup>1\*</sup>

<sup>1</sup>Department of Medicine (Cardiology), Klinikum rechts der Isar, Technische Universität München, Munich 81675, Germany; <sup>2</sup>Institute for Molecular Cell Biology, Medical Faculty, University Homburg/Saar, Universität des Saarlandes, Homburg/Saar 66421, Germany; <sup>3</sup>Department of Anatomy and Embryology, Leiden University Medical Center, Leiden 2333, The Netherlands; <sup>4</sup>DZHK (German Centre for Cardiovascular Research)—Partner Site Munich Heart Alliance, Munich 80802, Germany; and <sup>5</sup>Institute for Cardiovascular Prevention (IPEK), LMU München, Munich 80336, Germany

Received 6 February 2016; revised 18 March 2016; accepted 19 April 2016; online publish-ahead-of-print 16 June 2016

See page 302 for the editorial comment on this article (doi:10.1093/eurheartj/ehw380)

## Aims

Cardiomyocytes (CMs) generated from human induced pluripotent stem cells (hiPSCs) are increasingly used in disease modelling and drug evaluation. However, they are typically a heterogeneous mix of ventricular-, atrial-, and nodal-like cells based on action potentials (APs) and gene expression. This heterogeneity and the paucity of methods for high-throughput functional phenotyping hinder the full exploitation of their potential. We aimed at developing a method for rapid, sequential, and subtype-specific phenotyping of hiPSC-CMs with respect to AP morphology and single-cell arrhythmias.

## Methods and results

We used cardiac lineage-specific promoters to drive the expression of a voltage-sensitive fluorescent protein (VSFP-CR) in hiPSC-CMs, enabling subtype-specific optical AP recordings. In a patient-specific hiPSC model of long-QT syndrome type 1, AP prolongation and frequent early afterdepolarizations were evident in mutant ventricular- and atrial-like, but not in nodal-like hiPSC-CMs compared with their isogenic controls, consistent with the selective expression of the disease-causing gene. Furthermore, we demonstrate the feasibility of sequentially probing a cell over several days to investigate genetic rescue of the disease phenotype and to discern CM subtype-specific drug effects.

## Conclusion

By combining a genetically encoded membrane voltage sensor with promoters that drive its expression in the major subtypes of hiPSC-CMs, we developed a convenient system for disease modelling and drug evaluation in the relevant cell type, which has the potential to advance the emerging utility of hiPSCs in cardiovascular medicine.

## Keywords

Disease modelling • iPS cells • Cardiomyocyte subtypes • Optical action potential recordings

\* Corresponding author. I. Department of Medicine, Klinikum rechts der Isar, Technische Universität München, Ismaninger Str. 22, 81675 München, Germany. Tel: +49 89 4140 2350, Fax: +49 89 4140 4900, Email: amoretti@mytum.de (A.M.); Email: sinnecker@mytum.de (D.S.); Email: klaugwitz@mytum.de (K.-L.L.).

† These authors contributed equally to this article.

© The Author 2016. Published by Oxford University Press on behalf of the European Society of Cardiology.

This is an Open Access article distributed under the terms of the Creative Commons Attribution Non-Commercial License (<http://creativecommons.org/licenses/by-nc/4.0/>), which permits non-commercial re-use, distribution, and reproduction in any medium, provided the original work is properly cited. For commercial re-use, please contact journals.permissions@oup.com

## Translational perspective

Cardiomyocytes (CMs) generated from human induced pluripotent stem cells are an evolving platform to understand molecular disease mechanism and evaluate cardiovascular drugs. A major limitation of this system is that they represent a heterogeneous mix of ventricular-, atrial-, and nodal-like CMs. By expressing a voltage-sensitive fluorescent protein under the control of lineage-specific promoters, we developed a convenient system allowing high-throughput subtype-specific optical action potential (AP) imaging in these cells. This enables not only quantification of electrical phenotypes in patient-specific CMs but also subtype-specific investigation of drug effects, which may aid both drug development and safety pharmacology in the cardiovascular field.

## Introduction

Human induced pluripotent stem cells (hiPSCs) are already proved useful as platforms for studying disease mechanisms, pharmacological responses, and toxicology in patient- and healthy proband-cardiomyocytes (hiPSC-CMs).<sup>1,2</sup> These hiPSC-CMs are usually not derived as a homogenous population of cells but consist of different subtypes with ventricular-, atrial-, and nodal-like properties.<sup>3–5</sup> While this can be advantageous because it allows the study of physiology and disease mechanisms in all three major CM subtypes, it also poses a challenge, since phenotypes might be obscured by varying contributions of the different CM subtypes.

Although the development of subtype-specific differentiation protocols is making substantial progress,<sup>6–9</sup> it is still challenging to obtain pure populations of ventricular-, atrial-, or nodal-like hiPSC-CMs. Here, we used subtype-specific promoter fragments to drive expression of a voltage-sensitive fluorescent protein specifically in ventricular-, atrial-, and nodal-like hiPSC-derived CMs, respectively. Promoter-driven expression of this optical membrane potential sensor permits high-throughput membrane potential imaging in specific CM subtypes generated from healthy and diseased hiPSCs, thus allowing precise disease phenotyping and drug testing.

## Methods

Detailed methods are presented in Supplementary material online. Briefly, hiPSCs from a patient suffering from long-QT syndrome type 1 (LQT1) and from controls were generated and differentiated to CMs as previously described.<sup>4</sup> An isogenic control line was generated by correcting the LQT1 mutation by a homologous recombination approach. The membrane voltage sensor VSFP-CR (Addgene plasmid #40257) was expressed in hiPSC-CMs by a lentiviral expression system. In addition to the ubiquitous PGK promoter, different promoter constructs were subcloned into the lentiviral transfer plasmid to achieve subtype-specific expression. In hiPSC-CMs infected with these constructs, optical AP recordings at up to 500 Hz were performed using an epifluorescence microscope equipped with an image splitter projecting GFP and RFP emission to two separate regions of the chip of an sCMOS camera. The background-corrected RFP/GFP ratio served as a membrane potential signal. Action potential characteristics were calculated from an average of 6–10 subsequent APs. Data in the text and in bar graphs are presented as mean  $\pm$  95% confidence interval.

## Results

### Optical action potential recordings using a voltage-sensitive fluorescent protein

To enable promoter-driven subtype-specific membrane potential recordings in hiPSC-CMs, we initially established an optical imaging

system based on a genetically encoded, Förster resonance energy transfer (FRET)-mediated membrane potential sensor (voltage-sensitive fluorescent protein, VSFP), which has been developed to image electrical activity in neurons.<sup>10</sup> The sensor consists of a transmembrane voltage-sensing domain fused to a tandem of two fluorescent proteins (in this specific VSFP variant, termed VSFP-CR, the GFP variant clover, and the RFP variant mRuby2 are used), resulting in an FRET increase with membrane depolarization (Figure 1A). We first evaluated whether VSFP-CR could allow stable and prolonged detection of APs in hiPSC-CMs and used 3-month-old CMs derived by embryoid body (EB) differentiation of a healthy control hiPSC line, which we had previously characterized by patch-clamp electrophysiology.<sup>4</sup> Upon lentiviral gene transfer of the sensor to single dissociated CMs and expression under the ubiquitous PGK promoter, fluorescence from both clover GFP and mRuby2 RFP was clearly detected 72 h later (Figure 1B and D) in >95% of the cells (Supplementary material online, Figure S1A). As expected, VSFP-CR signal was not limited to any specific CM subtype, and VSFP-positive cells were found to express either the ventricular or the atrial or neither MLC2 isoform (Figure 1B and C). Importantly, VSFP-CR responded to membrane depolarization with a stable increase in the RFP/GFP emission ratio (Supplementary material online, Movie S1) and trains of APs could be optically recorded from infected CMs (Figure 1D and E), with AP durations (Figure 1F) in good agreement with the previously-reported current clamp recordings.<sup>4</sup>

### Cardiomyocyte subtype-specific expression of voltage-sensitive fluorescent protein

With the aim of expressing VSFP in an hiPSC-CM subtype-specific way, we performed a systematic single-cell-based functional and molecular screen to identify specific promoter elements allowing subtype-specific marking of hiPSC-CMs. Based on this screen and in agreement with previous work (see Supplementary material online, Results and Table S1), the *MLC2v*, *SLN*, and *SHOX2* transcripts appeared to be quite specifically expressed in ventricular-, atrial-, and nodal-like cells, respectively.

Therefore, we constructed lentiviral vectors encoding the VSFP sensor under the control of either an *MLC2v* enhancer (*MLC2v*-VSFP) or  $\sim$ 3.5 kb promoter elements preceding the *SLN* or *SHOX2* transcription start site (*SLN*-VSFP and *SHOX2*-VSFP, see Methods for details) and tested whether they will drive VSFP expression selectively in ventricular-, atrial-, and nodal-like hiPSC-CMs. Transduction efficiency, as assessed by quantitative polymerase chain reaction (PCR) on genomic DNA, was high for all lentiviral constructs and comparable with that of PGK-VSFP (see Supplementary material online, Results and Figure S1C). Five

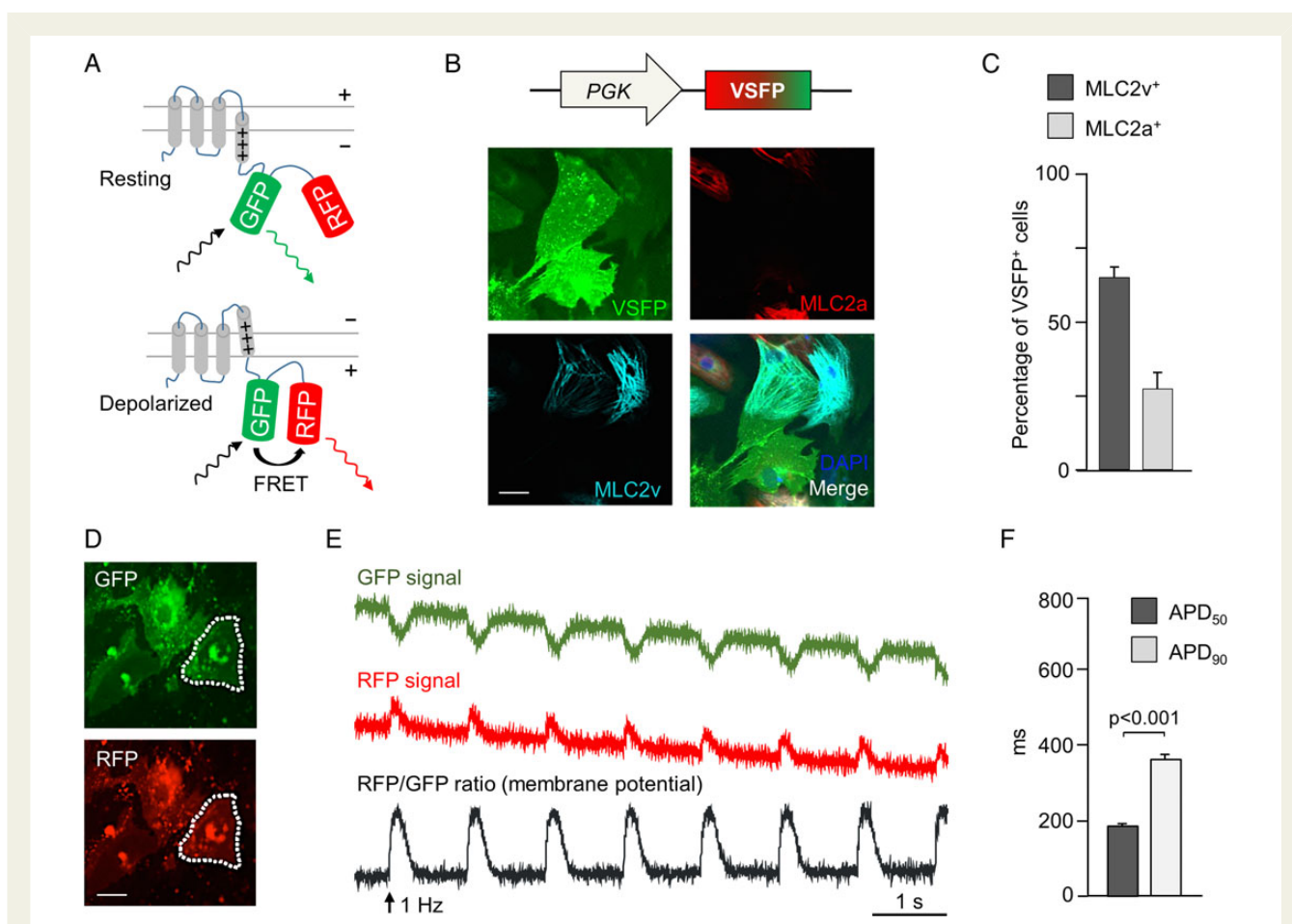


**Figure 1** Förster resonance energy transfer-based optical membrane potential recordings in human-induced pluripotent stem cells-derived cardiomyocytes. (A) Mode of action of the membrane potential sensor voltage-sensitive fluorescent protein. A voltage-sensing transmembrane protein is linked to a pair of a green and a red fluorescent protein. Upon depolarization, GFP and RFP are brought closer together, increasing Förster resonance energy transfer, which makes GFP appear dimmer and RFP brighter. (B) Pseudocolour images of human-induced pluripotent stem cells-derived cardiomyocytes infected with PGK-voltage-sensitive fluorescent protein lentivirus and stained for MLC2v (cyan) and MLC2a (red). (C) Percentage of cells expressing MLC2v and MLC2a among voltage-sensitive fluorescent protein-expressing cells ( $n = 325$  cells). (D) GFP and RFP pseudocolour images of voltage-sensitive fluorescent protein-expressing human-induced pluripotent stem cells-derived cardiomyocytes (dotted lines: region of interest used to quantify fluorescence signal). (E) Background-corrected GFP and RFP fluorescence signals recorded at 100 Hz upon field stimulation at 1 Hz. An RFP/GFP ratio was calculated as the membrane potential signal. (F) Action potential duration (APD<sub>50</sub> and APD<sub>90</sub>) in PGK-voltage-sensitive fluorescent protein-expressing cells.  $N = 92$  cells.

days after viral infection of single CMs dissociated from 3-month-old cardiac explants obtained by EB differentiation,<sup>11</sup> VSFP signal from each lentiviral construct was detectable (Figure 2A–C). MLC2v-VSFP was expressed in >70% of CMs, while SLN-VSFP and SHOX2-VSFP marked around 10 and 5% of the cell population, respectively (Supplementary material online, Figure S2B), consistent with the previously reported percentage of ventricular-, atrial-, and nodal-like subtypes in EB-differentiated iPSC-CMs.<sup>3,4</sup> Immunofluorescence analysis revealed that CMs positive for MLC2v-VSFP expressed the ventricular MLC2 isoform and, to a lesser extent, the atrial form (MLC2a). Expression of the transcription factor NKX2.5 specific for working myocardium was also widely observed, in contrast to expression of the atrial- and nodal-specific markers sarcolipin and SHOX2 (Figure 2A and D).

Most CMs marked by SLN-VSFP expressed the sarcoplasmic reticulum protein sarcolipin and also MLC2a and NKX2.5, consistent with an atrial-like phenotype (Figure 2B and D). In contrast, CMs labelled by the SHOX2 reporter expressed, in addition to the transcription factor SHOX2, the HCN4 channel and Podoplanin, another typical transmembrane protein of sinoatrial node cells (Figure 2C and D).

We further evaluated the specificity of our genetic marking strategy on the functional level (Figure 3). Optical AP recordings could be obtained from CMs infected with all three marker constructs at Day 7 post-transduction (Figure 3A–C). The AP duration (expressed as both APD<sub>50</sub> and APD<sub>90</sub>) was significantly longer in CMs expressing the MLC2v-VSFP when compared with those expressing the other two lentiviral constructs, consistent with a ventricular-like electrophysiological phenotype (Figure 3D). This was corroborated by a

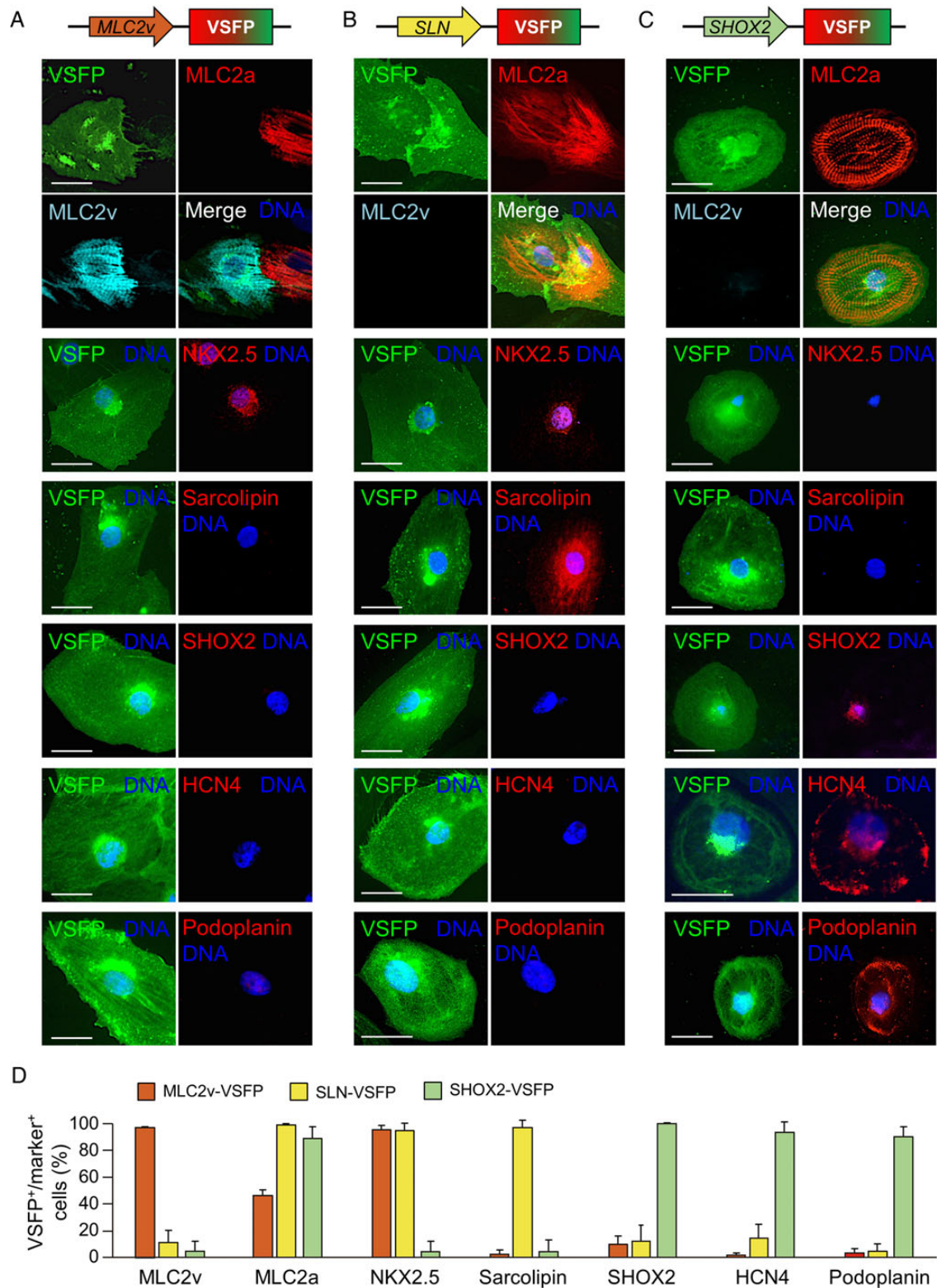


**Figure 2** Molecular characterization of cardiomyocytes marked with subtype-specific membrane potential sensor constructs. Typical pseudo-colour images of MLC2v-voltage-sensitive fluorescent protein- (A), SLN-voltage-sensitive fluorescent protein- (B), or SHOX2-voltage-sensitive fluorescent protein-infected (C) cells stained with the indicated antibodies. Scale bars: 20  $\mu$ m. (D) Percentage of voltage-sensitive fluorescent protein-positive cells expressing the indicated markers.  $N = 169-975$  cells for each marker.



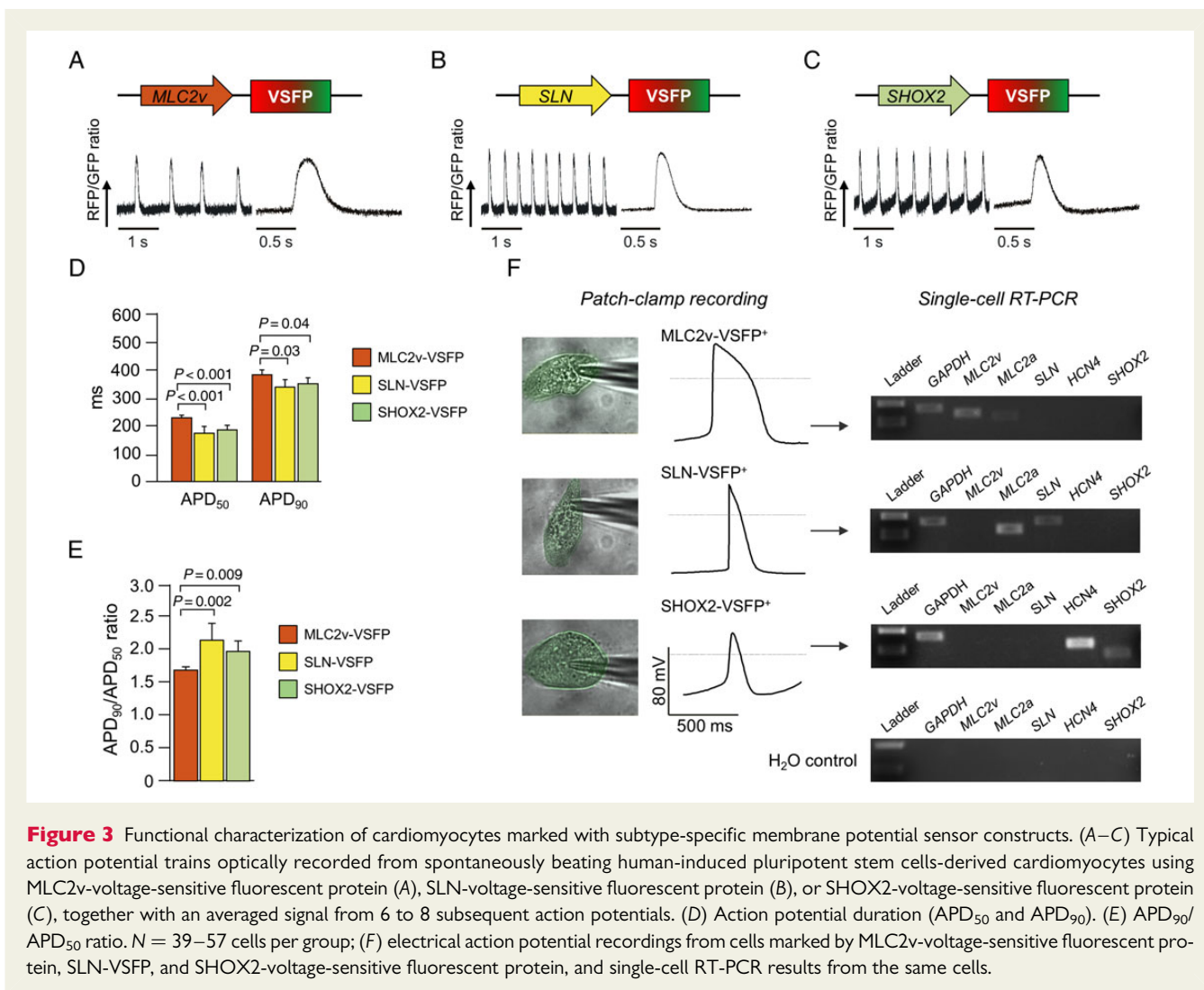


**Figure 3** Functional characterization of cardiomyocytes marked with subtype-specific membrane potential sensor constructs. (A–C) Typical action potential trains optically recorded from spontaneously beating human-induced pluripotent stem cells-derived cardiomyocytes using MLC2v-voltage-sensitive fluorescent protein (A), SLN-voltage-sensitive fluorescent protein (B), or SHOX2-voltage-sensitive fluorescent protein (C), together with an averaged signal from 6 to 8 subsequent action potentials. (D) Action potential duration (APD<sub>50</sub> and APD<sub>90</sub>). (E) APD<sub>90</sub>/APD<sub>50</sub> ratio.  $N = 39–57$  cells per group; (F) electrical action potential recordings from cells marked by MLC2v-voltage-sensitive fluorescent protein, SLN-VSFP, and SHOX2-voltage-sensitive fluorescent protein, and single-cell RT-PCR results from the same cells.

significantly lower APD<sub>90</sub>/APD<sub>50</sub> ratio (Figure 3E), which is also a typical finding in ventricular-like CMs.<sup>4</sup>

Similar results were obtained with additional iPSC lines generated from different somatic cell types (dermal fibroblasts and keratinocytes) using either retrovirus or sendai virus-mediated reprogramming (Supplementary material online, Figure S3). Moreover, the use of a chemically defined monolayer differentiation protocol yielding predominantly ventricular-like CMs resulted in a consistent distribution of CM subtypes based on marking with the different constructs (see Supplementary material online, Results and Figure S2B and C). These findings corroborate the robustness of our marking strategy.

Finally, in order to confirm the subtype identity of cells identified by each lentiviral construct, EB-differentiated CMs expressing VSFP were characterized by electrophysiological AP recordings and subsequent single-cell RT-PCR (Figure 3F). Cells positive for MLC2v-VSFP showed typical ventricular-like APs with a negative maximum diastolic potential, a rapid upstroke, and a pronounced plateau phase, and expressed *MLC2v*. Cells identified by SLN-VSFP exhibited typical AP properties of atrial-like CMs such as a fast upstroke velocity and a lack of a plateau phase, and expressed both,

*SLN* and *MLC2a*. Finally, SHOX2-VSFP-positive cells had a marked spontaneous diastolic depolarization and a slower upstroke velocity than the CMs marked by the other constructs, consistent with a nodal-like phenotype, which was corroborated by *SHOX2* and *HCN4* expression (see Figure 3F).

Taken together, these results indicate that our systems combining FRET-based VSFP and CM subtype-specific promoters allow selective optical AP measurements in ventricular-, atrial-, or nodal-like hiPSC-derived CMs.

### Cardiomyocyte subtype-specific investigation of long-QT syndrome

To further validate the feasibility of our method for quantitative short- and long-term assessment of AP prolongation and arrhythmogenic potential in CM subtypes, we used a patient-specific hiPSC model of LQT1. In this model, the heterozygous missense c.569G>A (p.R190Q) mutation in the potassium channel gene *KCNQ1* causes AP repolarization defects specifically in ventricular and atrial CMs, the two subtypes that express the mutated gene.<sup>4</sup> As control, in addition to the previously described hiPSC line

(CTR) obtained from an unrelated healthy volunteer without any cardiac disease,<sup>4</sup> we generated an isogenic line (LQT1<sup>corr</sup>) by correcting the KCNQ1-R190Q mutation in the patient LQT1<sup>R190Q</sup>-hiPSCs by classical homologous recombination (Figure 4A–D). This allowed us to eliminate effects of individual genetic background variability<sup>12</sup> and test whether the optical VSFP sensors could discern the net contribution of the disease-causing mutation to the LQT phenotype.

When we imaged APs of MLC2-VSFP-positive CMs electrically stimulated at 1 Hz, AP duration was significantly prolonged in diseased LQT1<sup>R190Q</sup> CMs when compared with the unmatched CTR CMs (APD<sub>90</sub> 616 ± 35 ms vs. 382 ± 17 ms;  $P < 0.01$ ;  $n = 72$  vs. 57 cells; Figure 4E) and consistent with previously reported patch-clamp recordings from the same cells<sup>4</sup> (see also Supplementary material online, Discussion). Importantly, a significant AP prolongation was also measured in mutated CMs when compared with the isogenic LQT1<sup>corr</sup> counterparts (APD<sub>90</sub> 474 ± 18 ms;  $P < 0.01$ ;  $n = 102$  cells). However, these cells had an almost 100 ms longer APD<sub>90</sub> than CTR CMs (Figure 4E). In accordance with the APD differences, the incidence of early afterdepolarizations (EADs)—spontaneous membrane depolarizations that occur before termination of the repolarization phase and can trigger ventricular arrhythmias<sup>13</sup>—was the highest in LQT1<sup>R190Q</sup> cells (22 ± 7%), significantly lower, but still present in LQT1<sup>corr</sup> cells (16 ± 7%), and almost absent in CTR cells (3 ± 3%) (Figure 4F). Similar results were obtained for the atrial lineage when membrane potentials were optically recorded in CMs from the same three hiPSC lines using the atrial-specific sensor SLN-VSFP (Figure 4G). In contrast, AP investigation in nodal-like CMs using SHOX2-VSFP showed no significant difference in APD<sub>50</sub> or APD<sub>90</sub> among LQT1<sup>R190Q</sup>, LQT1<sup>corr</sup>, and CTR lines (Figure 4G), corroborating previous findings from patch-clamp analysis in various hiPSC models of LQT1.<sup>4,14–16</sup>

These results demonstrate the ability of the subtype-specific VSFP sensors to detect and quantify genetically induced pathological changes in AP duration and prevalence of arrhythmic events in disease-relevant CM subtypes. Moreover, while proving the authenticity of the LQT1 genotype–phenotype correlation, they strongly suggest that the genetic background can affect the functional severity of LQT1-causing mutations.

## Measurements of dynamic changes in action potential duration in single cells over time

To further explore the versatility of VSFP for recording AP dynamics in hiPSC-CMs by repeated imaging of the same cell over time, we performed a rescue experiment. Here, the wild-type (wt) KCNQ1 ion channel subunit was overexpressed in the hiPSC-derived LQT1<sup>R190Q</sup> CMs by adeno-associated virus (AAV6)-mediated gene transfer (Figure 5A). The mutated KCNQ1 gene encodes a trafficking-deficient ion channel subunit that interacts with wild-type subunits and interferes with their integration into the plasma membrane, resulting in a dominant-negative effect,<sup>4</sup> which might be overcome by overexpression of wild-type subunits. Seven days after infection of LQT1<sup>R190Q</sup> CMs with MLC2v-VSFP lentivirus, APs were optically recorded and cells were subsequently infected with an AAV6 virus encoding wt KCNQ1 fused to the

haemagglutinin (HA) epitope tag (wt KCNQ1-HA AAV6) or a control virus encoding LacZ (LacZ-AAV6). Three days later (Day 10), APs were recorded again in the same cells and *post hoc* staining for the HA epitope and the β-gal transgene was performed to confirm viral transduction of the investigated cells (Figure 5A).

Indeed, wt KCNQ1 overexpression significantly shortened the APs of the LQT1<sup>R190Q</sup> CMs (Figure 5B and D), reaching APD values similar to those measured in LQT1<sup>corr</sup> cells. In contrast, no changes in APD were detectable in CMs infected with LacZ-AAV6 (Figure 4C and D). Thus, sequential AP imaging in the same cells using the MLC2v-VSFP sensor allowed detection of a successful LQT1 phenotype rescue in patient-derived hiPSC-CMs.

## Subtype-specific investigation of drug effects

Human induced pluripotent stem cell-derived CMs have been proposed to have utility in preclinical pharmacological assays. Specifically, allowing AP analysis in human CMs, they lend themselves to preclinical investigation of drug-induced QT interval prolongation. We therefore investigated whether our optical AP recording approach is applicable to assess such drug effects and whether it is suitable to assess subtype-specific pharmacological differences (Figure 5E–H).

We first studied the effects of cisapride, a prokinetic drug that is well known for inducing QT interval prolongation and Torsades de Pointes tachycardias in patients due to its potent ability to block hERG potassium channels. Since hERG channels are key determinants of the AP repolarization phase in all CM subtypes, we assumed that the PGK-VSFP sensor would be adequate for detecting drug-induced effects in a heterogeneous population of hiPSC-CMs. Indeed, by imaging the same PGK-VSFP-expressing cells before and after drug application, we measured a significant AP prolongation and increased prevalence of EADs in single CTR hiPSC-CMs treated with 100 nM cisapride (Figure 5F).

However, the ‘funny’ current ( $I_f$ ) inhibitor ivabradine, which is clinically used as a heart rate-reducing drug, showed no effect on overall beating frequency of CMs imaged using PGK-VSFP (Figure 5G), consistent with a previous report indicating that automaticity in ventricular-like hiPSC-CMs does not depend on  $I_f$ .<sup>17</sup> Ivabradine has a high selectivity for nodal cells, where the  $I_f$  current determines the pacemaker activity, and dramatically reduces the beating rate specifically in this CM subtype.<sup>18–20</sup> The absence of frequency reduction by 9 μM ivabradine in CTR cells marked by PGK-VSFP was likely due to the low percentage of nodal-like CMs in the cell population expressing the PGK promoter. Conversely, when the same treatment was applied to cells marked by MLC2v-VSFP, SLN-VSFP, or SHOX2-VSFP, cell automaticity was abolished exclusively in the SHOX2-VSFP-positive cells, with no effects on the other CM subtypes (Figure 5H), indicating the superiority of the subtype-specific systems for investigating pharmacological effects of drugs that act selectively on distinct CM lineages.

## Discussion

Human induced pluripotent stem cell-derived CMs are increasingly used to model cardiac diseases and hold promise for drug

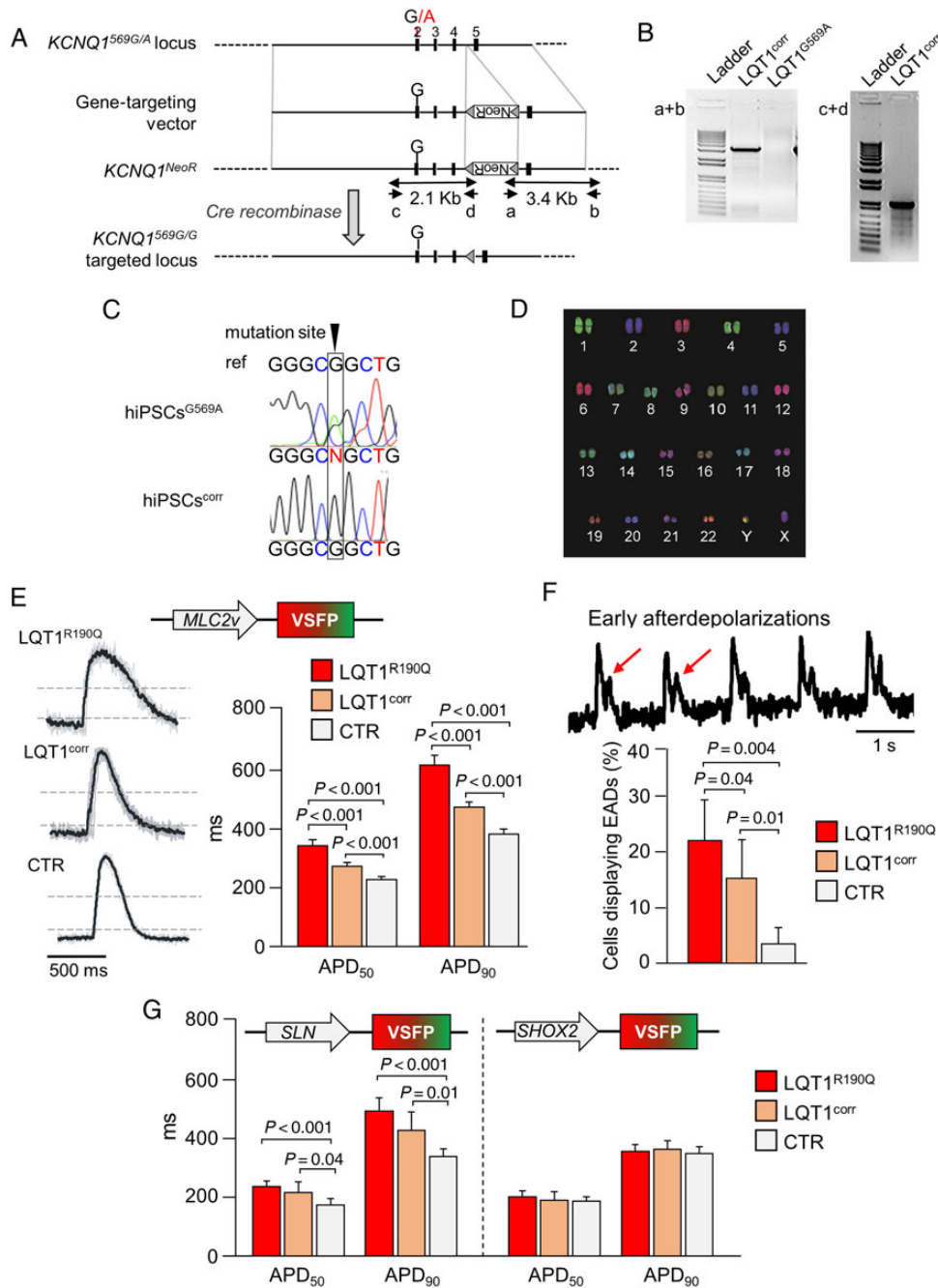


**Figure 4** Modelling long-QT syndrome using cardiomyocyte subtype-specific optical action potential recordings. (A) Gene-targeting strategy applied to correct the disease-causing *KCNQ1* mutation in LQT1 hiPSCs. (B) Polymerase chain reaction using primers a + b (3.4 kb) identified targeted clones while PCR using primers c + d (2.1 kb) followed by sequencing identified corrected clones. (C) Sanger sequencing demonstrated gene correction in the clonally isolated LQT1<sup>corr</sup> line. (D) Normal karyotype of the LQT1<sup>corr</sup> hiPSC line. (E–G) Optical action potential recordings from 1 Hz-paced cardiomyocytes generated from patient LQT1 human-induced pluripotent stem cells (LQT1<sup>R190Q</sup>), isogenic control (LQT1<sup>corr</sup>), and unrelated control (CTR) human-induced pluripotent stem cells infected with MLC2v-VSFP (E and F), SLN-VSFP, or SHOX2-voltage-sensitive fluorescent protein (G). (E) Typical optical action potential traces. Grey lines: single action potentials, black lines: averaged action potential. Dashed lines at 50 and 10% of action potential amplitude indicate where APD<sub>50</sub> and APD<sub>90</sub> were measured. APD<sub>50</sub> and APD<sub>90</sub> values in the three lines ( $n = 57–72$  cells per group) are shown. (F) Example of membrane potential recording showing early afterdepolarizations. Bar graph: percentage of cells exhibiting early afterdepolarizations ( $n = 57–72$  cells per group). (G) APD<sub>50</sub> and APD<sub>90</sub> values investigated using SLN-voltage-sensitive fluorescent protein and SHOX2-voltage-sensitive fluorescent protein as indicated ( $N = 20–65$  cells per group).

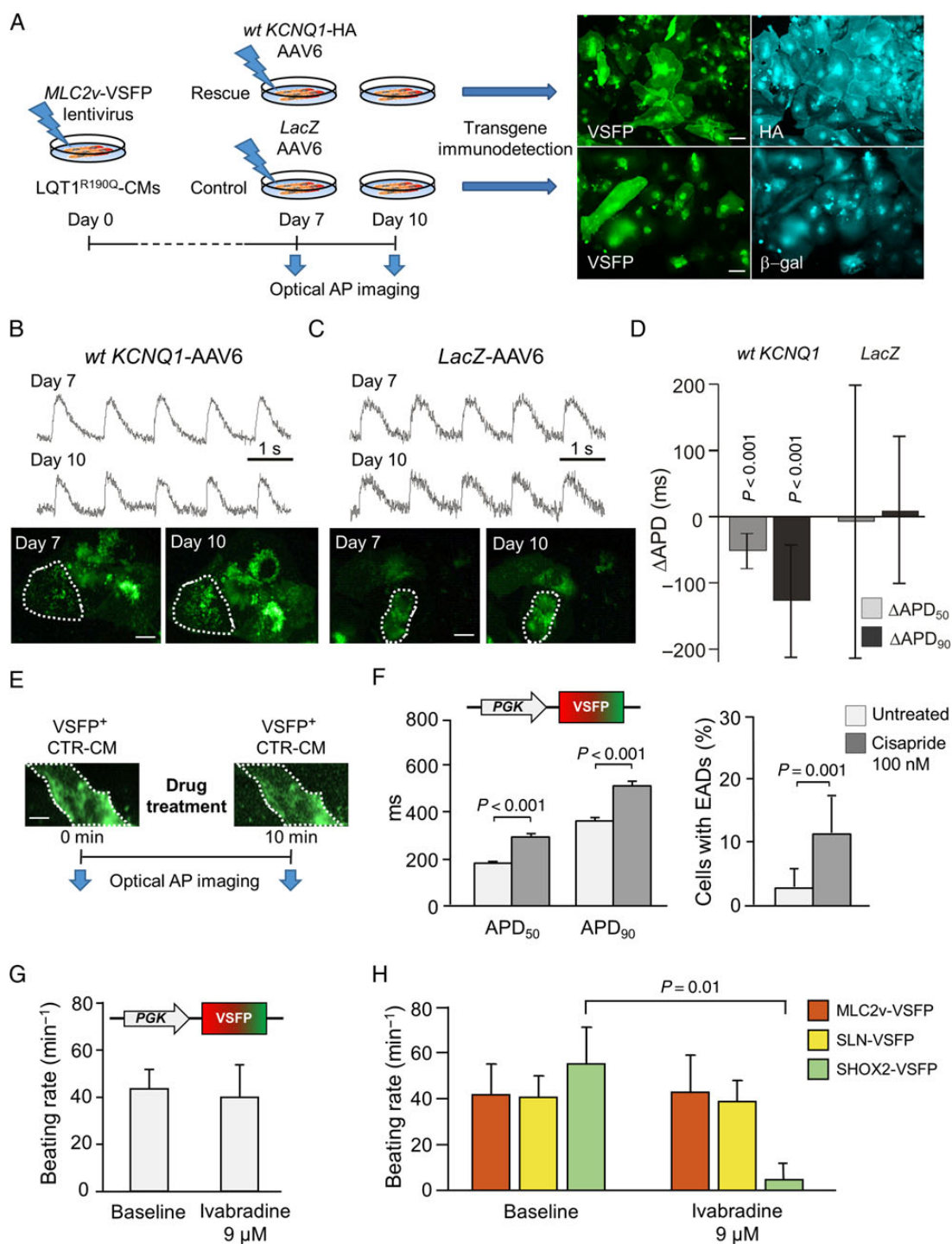


**Figure 5** Short- and long-term measurements of dynamic action potential changes: genetic rescue of LQT1 phenotype and subtype-specific drug effects. (A–D) Genetic rescue of the LQT1 phenotype. (A) Scheme of the rescue experiment. (B and C) Typical optical action potential tracings obtained from cells of the wild-type KCNQ1 (B) and control group (C) at Day 7 and at Day 10. Images: voltage-sensitive fluorescent protein green fluorescence at the indicated time points (dotted line: region of interest for fluorescence quantification). (D) Difference in action potential duration ( $\Delta$ APD<sub>50</sub> and  $\Delta$ APD<sub>90</sub>) at Day 10 compared with Day 7.  $N = 103$ –126 cells. (E–H) Optical investigation of drug-induced effects. (E) Experimental design. (F) APD<sub>50</sub> and APD<sub>90</sub> values (left) and the frequency of occurrence of early afterdepolarizations (right) before and after treatment with 100 nM Cisapride ( $n = 86$  cells). (G and H) CM subtype-specific effect of Ivabradine on the spontaneous beating rate. (G) Control cardiomyocytes expressing PGK-voltage-sensitive fluorescent protein were imaged before and after application of 9  $\mu$ M Ivabradine. (H) Control cardiomyocytes expressing MLC2v-voltage-sensitive fluorescent protein, SLN-voltage-sensitive fluorescent protein or SHOX2-voltage-sensitive fluorescent protein as indicated were imaged before and after application of 9  $\mu$ M Ivabradine.  $N = 11$ –18 cells per group.



development and toxicity assays investigating susceptibility to cardiac arrhythmias. However, their subtype heterogeneity poses a challenge for fulfilling their unique potential in the cardiovascular field.

In this study, we addressed the question of phenotyping the heterogeneous population of hiPSC-CMs by using a combination of a genetically encoded optical membrane potential sensor with promoter-driven genetic marking to record APs in a subtype-specific manner. The optical method not only increased the throughput far beyond that of single-cell patch-clamp electrophysiology, it also allowed sequential investigation of the same cells over extended time periods during genetic manipulation of AP dynamics. The subtype specificity substantially reduced the variability of AP properties caused by the heterogeneity in hiPSC-CMs differentiation and allowed investigation of phenotypes in a CM subtype-specific way.

In patient-derived hiPSC-CMs affected by congenital LQT1, we investigated key features of the disease such as AP prolongation and occurrence of EADs in a CM subtype-specific way. Moreover, employing a genetically corrected isogenic control line, we showed that the method is sensitive enough to detect the functional consequences of a single *KCNQ1-R190Q* mutation. A rescue experiment performed by overexpressing wild-type *KCNQ1* subunits in the patient cells highlighted the feasibility of repeated AP measurements in the same cells over time and, thus, long-term monitoring of AP dynamic changes. Finally, we demonstrated that our method allows assessment of the effects of QT interval-prolonging drugs such as cisapride on AP duration and the occurrence of EADs. Furthermore, the CM subtype specificity of the method makes possible a precise investigation of the response to pharmacological agents that have selective effects on atrial-, ventricular-, and/or pacemaker-like cells, as we proved for the  $I_f$  current inhibitor ivabradine.

Since their introduction in 2007,<sup>21,22</sup> hiPSCs have been extensively used to model cardiac diseases, with a strong focus on channelopathies.<sup>2,23</sup> Another focus of intensive research is the integration of these cells into preclinical drug safety assays, particularly to assess QT interval prolongation.<sup>14,24–29</sup> While patch-clamp electrophysiology is the gold standard to assess electrical properties of hiPSC-CMs, it suffers from the major limitation of a very limited throughput, which is further restricted by the necessity to identify the CM subtype of interest based on AP morphology.<sup>4,14–16</sup>

Optical AP recordings are an emerging tool to overcome this limitation.<sup>30</sup> Using genetically encoded voltage sensors, APs were imaged in rat primary CMs,<sup>31</sup> whole mouse hearts,<sup>32</sup> and human embryonic stem cell-derived CMs.<sup>33</sup> Optical AP imaging was recently conducted successfully in hiPSC-CMs using the genetically encoded voltage indicator ArcLight.<sup>34,35</sup> In contrast to the VSFP-CR sensor, ArcLight does not provide a ratiometric readout, making it more susceptible to cell movement artefacts and photobleaching. By expressing VSFP-CR under promoter fragments specifically expressed in ventricular-, atrial-, and nodal-like hiPSC-CMs, we could refine the optical AP measurement method with a CM subtype-specific component.

Despite their advantages, optically recorded membrane potential measurements are not equivalent to classical patch-clamp recordings. They do not allow absolute quantification of transmembrane potentials yet, and the AP signal is influenced by the kinetics of the VSFP conformational change (see Supplementary material online,

Discussion). Nevertheless, the system is sensitive and precise enough to detect the AP prolongation caused by a single potassium channel gene mutation and to detect single-cell arrhythmias such as EADs.

In summary, we developed a convenient system for subtype-specific AP imaging in hiPSC-CMs that has the potential to advance the emerging utility of hiPSCs in cardiovascular medicine and drug development.

## Supplementary material

Supplementary material is available at *European Heart Journal* online.

## Acknowledgements

We thank C. Scherb, D. Grewe, and B. Campbell for expert technical assistance, R.P. Davis for help in designing the *KCNQ1* gene-targeting strategy, and M.J.M. van der Burg, K. Szuhai, and H. Tanke for karyotyping analysis.

## Funding

This work was supported by grants from the European Research Council, MEXT-23208 and ERC 261053 (K.-L.L.); the German Research Foundation, Research Unit 923, Mo 2217/1-1 (A.M.), La 1238 3-1/4-1/4-2 (K.-L.L.); Si 1747/1-1 (D.S.); Transregio Research Unit 152 (A.M., K.-L.L., and P.L.); EU Marie Curie FP7-People-2011-IEF Programme, HPSCLQT 29999 (M.B.); the Netherlands Institute of Regenerative Medicine (C.L.M.); the Else Kröner-Fresenius-Stiftung (D.S.). Funding to pay the Open Access publication charges for this article was provided by the European Research Council.

**Conflict of interest:** none declared.

## References

- Bellin M, Marchetto MC, Gage FH, Mummery CL. Induced pluripotent stem cells: the new patient? *Nat Rev Mol Cell Biol* 2012;**13**:713–726.
- Moretti A, Laugwitz KL, Dorn T, Sinnecker D, Mummery C. Pluripotent stem cell models of human heart disease. *Cold Spring Harb Perspect Med* 2013;**3** doi: 10.1101/cshperspect.a014027.
- Zhang J, Wilson GF, Soerens AG, Koonce CH, Yu J, Palecek SP, Thomson JA, Kamp TJ. Functional cardiomyocytes derived from human induced pluripotent stem cells. *Circ Res* 2009;**104**:e30–e41.
- Moretti A, Bellin M, Welling A, Jung CB, Lam JT, Bott-Flugel L, Dorn T, Goedel A, Hohnke C, Hofmann F, Seyfarth M, Sinnecker D, Schomig A, Laugwitz KL. Patient-specific induced pluripotent stem-cell models for long-QT syndrome. *N Engl J Med* 2010;**363**:1397–1409.
- Ma J, Guo L, Fiene SJ, Anson BD, Thomson JA, Kamp TJ, Kolaja KL, Swanson BJ, January CT. High purity human-induced pluripotent stem cell-derived cardiomyocytes: electrophysiological properties of action potentials and ionic currents. *Am J Physiol Heart Circ Physiol* 2011;**301**:H2006–H2017.
- Zhu WZ, Xie Y, Moyes KW, Gold JD, Askari B, Laflamme MA. Neuregulin/ErbB signaling regulates cardiac subtype specification in differentiating human embryonic stem cells. *Circ Res* 2010;**107**:776–786.
- Zhang Q, Jiang J, Han P, Yuan Q, Zhang J, Zhang X, Xu Y, Cao H, Meng Q, Chen L, Tian T, Wang X, Li P, Hescheler J, Ji G, Ma Y. Direct differentiation of atrial and ventricular myocytes from human embryonic stem cells by alternating retinoid signals. *Cell Research* 2011;**21**:579–587.
- Devalla HD, Schwach V, Ford JW, Milnes JT, El-Haou S, Jackson C, Gkatzis K, Elliott DA, Chuva de Sousa Lopes SM, Mummery CL, Verkerk AO, Passier R. Atrial-like cardiomyocytes from human pluripotent stem cells are a robust preclinical model for assessing atrial-selective pharmacology. *EMBO Mol Med* 2015;**7**:394–410.
- Birket MJ, Ribeiro MC, Verkerk AO, Ward D, Leitoguinho AR, den Hartogh SC, Orlova VV, Devalla HD, Schwach V, Bellin M, Passier R, Mummery CL. Expansion and patterning of cardiovascular progenitors derived from human pluripotent stem cells. *Nat Biotechnol* 2015;**33**:970–979.
- Lam AJ, St-Pierre F, Gong Y, Marshall JD, Cranfill PJ, Baird MA, McKeown MR, Wiedenmann J, Davidson MW, Schnitzer MJ, Tsien RY, Lin MZ. Improving FRET

- dynamic range with bright green and red fluorescent proteins. *Nat Methods* 2012;**9**: 1005–1012.
11. Gramlich M, Pane LS, Zhou Q, Chen Z, Murgia M, Schotterl S, Goedel A, Metzger K, Brade T, Parrotta E, Schaller M, Gerull B, Thierfelder L, Aartsma-Rus A, Labeit S, Atherton JJ, McGaughan J, Harvey RP, Sinnecker D, Mann M, Laugwitz KL, Gawaz MP, Moretti A. Antisense-mediated exon skipping: a therapeutic strategy for titin-based dilated cardiomyopathy. *EMBO Mol Med* 2015;**7**:562–576.
  12. Bellin M, Casini S, Davis RP, D'Aniello C, Haas J, Ward-van Oostwaard D, Tertoolen LG, Jung CB, Elliott DA, Welling A, Laugwitz KL, Moretti A, Mummery CL. Isogenic human pluripotent stem cell pairs reveal the role of a KCNH2 mutation in long-QT syndrome. *EMBO J* 2013;**32**:3161–3175.
  13. Volders PG, Vos MA, Szabo B, Sipido KR, de Groot SH, Gorgels AP, Wellens HJ, Lazzara R. Progress in the understanding of cardiac early afterdepolarizations and torsades de pointes: time to revise current concepts. *Cardiovasc Res* 2000;**46**: 376–392.
  14. Liang P, Lan F, Lee AS, Gong T, Sanchez-Freire V, Wang Y, Diecke S, Sallam K, Knowles JW, Wang PJ, Nguyen PK, Bers DM, Robbins RC, Wu JC. Drug screening using a library of human induced pluripotent stem cell-derived cardiomyocytes reveals disease-specific patterns of cardiotoxicity. *Circulation* 2013;**127**:1677–1691.
  15. Wang Y, Liang P, Lan F, Wu H, Lisowski L, Gu M, Hu S, Kay MA, Urnov FD, Shinawi R, Gold JD, Gepstein L, Wu JC. Genome editing of isogenic human induced pluripotent stem cells recapitulates long QT phenotype for drug testing. *J Am Coll Cardiol* 2014;**64**:451–459.
  16. Ma D, Wei H, Lu J, Huang D, Liu Z, Loh LJ, Islam O, Liew R, Shim W, Cook SA. Characterization of a novel KCNQ1 mutation for type 1 long QT syndrome and assessment of the therapeutic potential of a novel IKs activator using patient-specific induced pluripotent stem cell-derived cardiomyocytes. *Stem Cell Res Ther* 2015;**6**:39.
  17. Kim JJ, Yang L, Lin B, Zhu X, Sun B, Kaplan AD, Bett GC, Rasmusson RL, London B, Salama G. Mechanism of automaticity in cardiomyocytes derived from human induced pluripotent stem cells. *J Mol Cell Cardiol* 2015;**81**:81–93.
  18. Dorn T, Goedel A, Lam JT, Haas J, Tian Q, Herrmann F, Bundschu K, Dobrova G, Schiemann M, Dirschingner R, Guo Y, Kuhl SJ, Sinnecker D, Lipp P, Laugwitz KL, Kuhl M, Moretti A. Direct nkx2-5 transcriptional repression of *isl1* controls cardiomyocyte subtype identity. *Stem Cells* 2015;**33**:1113–1129.
  19. Thollon C, Cambarrat C, Vian J, Prost JF, Peglion JL, Vilaine JP. Electrophysiological effects of S 16257, a novel sino-atrial node modulator, on rabbit and guinea-pig cardiac preparations: comparison with UL-FS 49. *Br J Pharmacol* 1994;**112**:37–42.
  20. Barbuti A, Crespi A, Capilupo D, Mazzocchi N, Baruscotti M, DiFrancesco D. Molecular composition and functional properties of f-channels in murine embryonic stem cell-derived pacemaker cells. *J Mol Cell Cardiol* 2009;**46**:343–351.
  21. Takahashi K, Tanabe K, Ohnuki M, Narita M, Ichisaka T, Tomoda K, Yamanaka S. Induction of pluripotent stem cells from adult human fibroblasts by defined factors. *Cell* 2007;**131**:861–872.
  22. Yu J, Vodyanik MA, Smuga-Otto K, Antosiewicz-Bourget J, Frane JL, Tian S, Nie J, Jonsdottir GA, Ruotti V, Stewart R, Slukvin I, Thomson JA. Induced pluripotent stem cell lines derived from human somatic cells. *Science* 2007;**318**:1917–1920.
  23. Yang C, Al-Aama J, Stojkovic M, Keavney B, Trafford A, Lako M, Armstrong L. Concise review: cardiac disease modeling using induced pluripotent stem cells. *Stem Cells* 2015;**33**:2643–2651.
  24. Tanaka T, Tohyama S, Murata M, Nomura F, Kaneko T, Chen H, Hattori F, Egashira T, Seki T, Ohno Y, Koshimizu U, Yuasa S, Ogawa S, Yamanaka S, Yasuda K, Fukuda K. In vitro pharmacologic testing using human induced pluripotent stem cell-derived cardiomyocytes. *Biochem Biophys Res Commun* 2009;**385**: 497–502.
  25. Mehta A, Chung Y, Sequiera GL, Wong P, Liew R, Shim W. Pharmacoelectrophysiology of viral-free induced pluripotent stem cell-derived human cardiomyocytes. *Toxicol Sci* 2013;**131**:458–469.
  26. Navarrete EG, Liang P, Lan F, Sanchez-Freire V, Simmons C, Gong T, Sharma A, Burrig PW, Patlolla B, Lee AS, Wu H, Beygui RE, Wu SM, Robbins RC, Bers DM, Wu JC. Screening drug-induced arrhythmia using human induced pluripotent stem cell-derived cardiomyocytes and low-impedance microelectrode arrays. *Circulation* 2013;**128**(11 Suppl. 1):S3–S13.
  27. Sager PT, Gintant G, Turner JR, Pettit S, Stockbridge N. Rechanneling the cardiac proarrhythmia safety paradigm: a meeting report from the Cardiac Safety Research Consortium. *Am Heart J* 2014;**167**:292–300.
  28. Scheel O, Frech S, Amuzescu B, Eisfeld J, Lin KH, Knott T. Action potential characterization of human induced pluripotent stem cell-derived cardiomyocytes using automated patch-clamp technology. *Assay Drug Dev Technol* 2014;**12**: 457–469.
  29. Sinnecker D, Laugwitz KL, Moretti A. Induced pluripotent stem cell-derived cardiomyocytes for drug development and toxicity testing. *Pharmacol Ther* 2014;**143**: 246–252.
  30. Kaestner L, Tian Q, Kaiser E, Xian W, Muller A, Oberhofer M, Ruppenthal S, Sinnecker D, Tsutsui H, Miyawaki A, Moretti A, Lipp P. Genetically encoded voltage indicators in circulation research. *Int J Mol Sci* 2015;**16**:21626–21642.
  31. Tian Q, Oberhofer M, Ruppenthal S, Scholz A, Buschmann V, Tsutsui H, Miyawaki A, Zeug A, Lipp P, Kaestner L. Optical action potential screening on adult ventricular myocytes as an alternative QT-screen. *Cell Physiol Biochem* 2011;**27**: 281–290.
  32. Chang Liao ML, de Boer TP, Mutoh H, Raad N, Richter C, Wagner E, Downie BR, Unsold B, Arooj I, Streckfuss-Bomeke K, Doker S, Luther S, Guan K, Wagner S, Lehnart SE, Maier LS, Stuhmer W, Wettwer E, van Veen T, Morlock MM, Knopfel T, Zimmermann WH. Sensing cardiac electrical activity with a cardiac myocyte – targeted optogenetic voltage indicator. *Circ Res* 2015;**117**:401–412.
  33. Leyton-Mange JS, Mills RW, Macri VS, Jang MY, Butte FN, Ellinor PT, Milan DJ. Rapid cellular phenotyping of human pluripotent stem cell-derived cardiomyocytes using a genetically encoded fluorescent voltage sensor. *Stem Cell Reports* 2014;**2**: 163–170.
  34. Song L, Awari DW, Han EY, Uche-Anya E, Park SH, Yabe YA, Chung WK, Yazawa M. Dual optical recordings for action potentials and calcium handling in induced pluripotent stem cell models of cardiac arrhythmias using genetically encoded fluorescent indicators. *Stem Cells Transl Med* 2015;**4**:468–475.
  35. Shinawi R, Huber I, Maizels L, Shaheen N, Gepstein A, Arbel G, Tijssen AJ, Gepstein L. Monitoring human-induced pluripotent stem cell-derived cardiomyocytes with genetically encoded calcium and voltage fluorescent reporters. *Stem Cell Reports* 2015;**5**:582–596.